UC-404

LBL-29191
Preprint

Center for Advanced Materials

CAM

Submitted to Surface Science

The Surface Oxidation of Alpha-Silicon Carbide by O_2 from 300K to 1373K

J.M. Powers and G.A. Somorjai

October 1990

For Reference

Not to be taken from this room

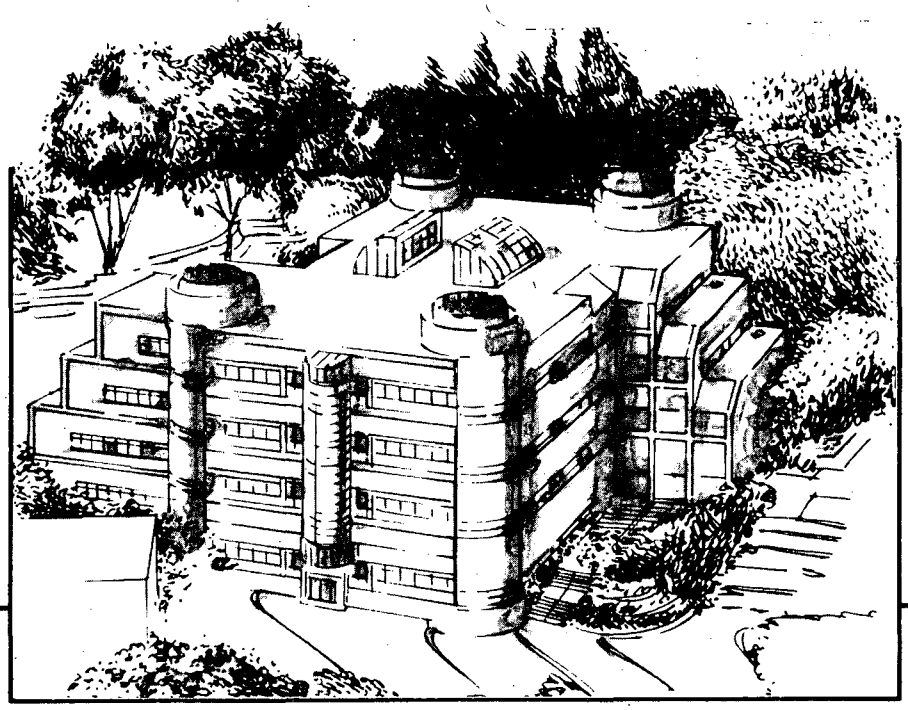

Materials and Chemical Sciences Division

Lawrence Berkeley Laboratory • University of California

ONE CYCLOTRON ROAD, BERKELEY, CA 94720 • (415) 486-4755

Prepared for the U.S. Department of Energy under Contract DE-AC03-76SF00098

LBL-29191
Copy 1
Bldg. 50 Library.

DISCLAIMER

This document was prepared as an account of work sponsored by the United States Government. While this document is believed to contain correct information, neither the United States Government nor any agency thereof, nor the Regents of the University of California, nor any of their employees, makes any warranty, express or implied, or assumes any legal responsibility for the accuracy, completeness, or usefulness of any information, apparatus, product, or process disclosed, or represents that its use would not infringe privately owned rights. Reference herein to any specific commercial product, process, or service by its trade name, trademark, manufacturer, or otherwise, does not necessarily constitute or imply its endorsement, recommendation, or favoring by the United States Government or any agency thereof, or the Regents of the University of California. The views and opinions of authors expressed herein do not necessarily state or reflect those of the United States Government or any agency thereof or the Regents of the University of California.

LBL-29191

The Surface Oxidation of Alpha-Silicon Carbide by O_2 from 300K to 1373K

James M. Powers and Gabor A. Somorjai

June 15, 1990

Materials Science Division
Center for Advanced Materials
Lawrence Berkeley Laboratory
University of California
Berkeley, CA 94720 U.S.A.

and

Department of Chemistry
University of California
Berkeley, CA 94720 U.S.A.

ACKNOWLEDGMENT
This work was supported by the Director, Office of Energy Research, Office of Basic Energy Sciences, Material Sciences Division, U.S. Department of Energy under contract No. DE-AC03--76SF00098.

Abstract:

Auger Electron Spectroscopy (AES), Low Energy Electron Diffraction (LEED), and X-Ray Photoelectron Spectroscopy (XPS) were used to investigate the oxidation of single crystal α-SiC over a wide temperature and O_2 pressure range. In ultra-high vacuum, the surface composition of α-SiC $(000\bar{1})$ as a function of temperature changes due to oxide formation and the sublimation of SiO and Si, yielding graphitic surface carbon. From 300K to 833K, exposure of Ar^+ bombarded α-SiC to 10^{-8} Torr O_2 results in a two stage oxidation process which yields a submonolayer oxide. Highly disordered α-SiC surfaces were found to oxidize faster and more extensively than well annealed, ordered surfaces. Exposure of the α-SiC{0001} surfaces to 1 atm O_2 resulted in the production of SiO_2 overlayers, which were examined using XPS and Scanning AES (SAES). In these experiments the $(000\bar{1})$ surface produced thicker SiO_2 overlayers than the (0001) surface. However, the difference in oxide thickness between the two {0001} surfaces was not as dramatic as previously reported and varied from sample to sample. Carbon was not detected in the surface SiO_2 layers formed between 873K and 1373K, which suggested carbon was removed as CO and/or CO_2 during the SiC oxidation process.

Introduction:

In recent years, methods have been developed to reproducibly grow high quality single crystals of silicon carbide [1,2]. Both the hexagonal and cubic forms of SiC (α and β, respectively) are large bandgap ceramic semiconductors that can be doped p or n-type. The large bandgap makes possible the use of both forms in high temperature electrical applications. In addition, the chemical inertness and extreme hardness of SiC (9.2 on Mohs scale) make it an excellent structural ceramic for use in harsh environments.

For SiC to fulfill its potential as an electronic material, methods must be developed to produce insulating oxide layers on SiC surfaces in a reproducible fashion. The study of the surface oxidation process should take into account the crystallographic polarity of SiC, since both the surface symmetry and atomic composition depend on the orientation of the surface examined. For α-SiC, the ideal $(000\bar{1})$ basal surface is terminated in carbon atoms, while the (0001) basal surface is terminated in silicon atoms. (see fig. 1) A method for determining the identity of these two surfaces via chemical etching was developed by Brack using x-ray dispersion effects [3].

Studies of the high temperature oxidation of these basal surfaces by O_2 have shown the two surfaces have significantly different oxidation rates. Harris and Call found that exposure of single crystal α-SiC to one atmosphere of O_2 for 70 hours at 1,333K produced 900 Å of SiO_2 on one basal surface, and 6,500 Å on the other [4]. Suzuki et al. found very similar results for the oxidation of α-SiC [5]. Exposure of

α-SiC at 1273K to H_2O saturated O_2 (P=1 atm) for two hours produced 152 Å SiO_2 on the (0001) surface, 908 Å SiO_2 on the $(000\bar{1})$ surface, and for comparison, 1949 Å SiO_2 on a Si (111) surface.

While these studies provide valuable information on the macroscopic oxidation of α-SiC, they are unable to address the questions of surface composition and structure during the initial stages of oxidation. Muehlhoff and coworkers utilized a combination of X-ray Photoelectron Spectroscopy (XPS), Auger Electron Spectroscopy (AES), and Energy-Loss Spectroscopy (ELS) to analyze the {0001} surfaces of α-SiC as a function of temperature [6] and O_2 exposure [7]. In ultra high vacuum (UHV) both {0001} surfaces showed carbon enrichment of the surface region at elevated temperatures. The $(000\bar{1})$ surface showed enrichment as low as 900K, while the (0001) surface composition was stable up to 1300K, at which point surface graphitization took place. This graphitization process at 1300K occurred on both surfaces and was attributed to silicon evaporation from the surface region. Surface carbon enrichment appeared to be an important factor in the oxidation of the {0001} surfaces by O_2. Utilizing an O_2 exposure pressure of 54 mTorr, Muehlhoff et. al. compared the oxidation rates of both surfaces at 995K and 1345K. At both temperatures, the $(000\bar{1})$ surface oxidized at a faster rate than the (0001) surface. However, for short O_2 exposure times the extent of oxidation on both surfaces was less at 1345K than at 995K. At 1345K, graphite from the thermal decomposition of α-SiC covered both {0001} surfaces. The authors proposed that once this graphite was removed by a sufficient exposure to O_2, a second oxidation process took over with a much higher rate than that was seen at 995K. For

both {0001} surfaces, no evidence of C-O surface bonding was observed.

Our work has utilized a wide temperature and O_2 pressure range in order to study the surface oxidation process of single crystal α-SiC from the initial stages of oxide growth to the production of thick oxide layers. Utilizing AES, XPS, and Low Energy Electron Diffraction (LEED), we explored the α-SiC surface composition in UHV as a function of temperature. The interaction of the basal surfaces of α-SiC with O_2 at 10^{-8} Torr was explored, and surface graphitization due to SiO and Si sublimation is discussed. The effect of surface roughness on the rate of oxidation was examined. The relatively slow oxidation of an ordered $(000\bar{1})$ surface at 973K is attributed to the crystallographic orientation of the surface and a lack of sites suitable for oxygen bonding.

The production of thick SiO_2 layers obtained at high O_2 partial pressures was examined using Scanning Auger Electron Spectroscopy (SAES) and Scanning Electron Microscopy (SEM). The composition of both α-SiC {0001} surfaces was examined after exposing the crystal to 1 atm of O_2 for 1 hour at various temperatures. Exposure of α-SiC to O_2 at 300K and 573K resulted in the production of thin SiO_x ($x<2$) surface layers, while O_2 exposure from 873K to 1373K produced surface SiO_2. To study the effect of surface polarity on the production of thick SiO_2 overlayers, multiple α-SiC samples at 1323K were exposed to 1 atm of flowing O_2 for one hour. For all the crystals utilized, the $(000\bar{1})$ surface produced thicker oxide layers than the (0001) surface under identical conditions. However, the difference between the two surfaces was considerably less than previously reported and also appeared to

be sample dependent. In addition, the thickness of the SiO_2 layer on each basal surface varied over the exposed surface area of the crystal.

Experimental:

Three UHV chambers were used for the α-SiC surface analysis. A Varian chamber with a base pressure of $5x10^{-10}$ torr was utilized for AES, LEED, and mass spectroscopic analysis. The α-SiC crystals were mounted on an off-axis manipulator and were heated either resistively or by electron bombardment. Surface cleaning was performed with glancing angle 400 eV Ar^+ bombardment with simultaneous annealing, yielding a clean surface with the exception of small amounts of embedded argon and surface oxygen. After cleaning the surface was exposed to O_2 by backfilling the entire chamber through a Varian leak valve. The O_2 exposure was measured in Langmuirs with the chamber pressure being read with an uncorrected ion gauge. A PHI single pass cylindrical mirror analyzer was used for AES with a primary beam energy of 1500eV. Consecutive AES scans yielded peak to peak intensities that were reproducible within 3%. A PHI 4-grid LEED/Auger optics system was utilized for LEED studies, and the residual gas load of the chamber was analyzed with an Extrel quadrapole mass spectrometer.

The second chamber utilized was a PHI 5300 ESCA system with a base pressure of $2x10^{-10}$torr. The system is equipped with a hemispherical energy analyzer (37.75 eV pass energy) and Mg X-ray source. (Mg Kα X-ray: 1253.6 eV) Sample cleaning was performed by 3kV Ar^+ bombardment at room temperature.

To produce thick oxide layers on α-SiC, crystals were exposed to 1 atm of flowing O_2 in a quartz tube furnace. The crystals were placed into the preheated tube, the tube was pumped to 10^{-4} torr with a turbo pump, and then O_2 was flowed into the system at approximately 200 cm^3/min.

A PHI 660 Scanning Auger Multiprobe was utilized for the SAES and SEM studies of the oxide layers on α-SiC produced via O_2 exposure at 1 atm. A primary beam energy of 3 kV was typically used for AES and SEM analysis. Images of the oxide layer with a magnification of greater than 400x were unattainable via SEM due to charging in the oxide layer. Argon ion depth profiling was performed at 5 kV over a rastered 3mm x 3mm area. Both basal surfaces of each crystal were analyzed with each surface being analyzed in 3 separate areas. Multiple analysis areas were utilized to check the uniformity of the surface oxide layer. The average of these values is reported as the oxide thickness. It was assumed the SiO_2/SiC interface had been reached when the oxygen AES intensity declined to one half its value in the SiO_2 bulk. The sputter rate was calibrated by measuring the time required to remove a known thickness of SiO_2 from a polished Si(111) wafer. The SiO_2 thickness on the Si(111) wafer was first determined by ellipsometry and interferometry. After the experiments the orientation of the α-SiC basal surfaces ((0001) vs. $(000\bar{1})$) was determined by etching the crystals for 10 minutes in molten Na_2CO_3 at 1220K. After etching, an examination of the (0001) surface with an optical microscope revealed numerous distorted hexagonal etch pits, while the $(000\bar{1})$ surface appeared wormy (See fig. 2)

For the AES/LEED studies the crystals were rinsed with distilled water, methanol, acetone, and 49% HF before mounting in UHV. The HF was utilized to remove the native oxide layer. To avoid charging during electron or Ar^+ bombardment the crystals were usually attached to

tantalum using a 90% Au/10% Ta alloy. A 0.1 mm foil of the alloy was placed between the α-SiC crystal and the tantalum substrate, and then the entire arrangement was heated to approximately 1600K in vacuum for 5 minutes. This melted the alloy and provided an ohmic contact between the α-SiC and tantalum substrate. The temperature of the crystal was determined with a chromel-alumel thermocouple. The thermocouple was spotwelded to a piece of 0.1 mm tantalum foil. The thermocouple and foil were either mechanically held against the crystal surface or were bonded to the crystal surface using the Au/Ta alloy.

Two types of single crystal α-SiC samples were utilized in the experiments Crystals prepared in commercial furnaces used for the manufacturing. of SiC abrasive were obtained from Atomergic Chemetals Company. These crystals will be referred to as the "commercial" samples. Due to the poor crystallinity of these samples, no LEED diffraction patterns were obtainable. Higher quality α-SiC crystals provided by W. J. Choyke [(a)] were also utilized in these experiments. Produced by the Lely method, these crystals were n-type semiconductors and the basal surfaces provided LEED patterns without any mechanical polishing.

The extent of surface oxidation was determined by measuring the peak to peak heights (I(X)) of the differentiated Si(LVV), C(KLL), and O(KLL) AES signals. The Si(LVV) transition was chosen since it is most sensitive to the presence of surface oxygen. In SiC, the Si(LVV) AES transition produces an intense peak at 89 eV. As oxygen bonds to the SiC surface, I(Si) declines monotonically. In SiO_2, this 89 eV peak is reduced to just a shoulder on the main LVV peak at 76 eV.

(a) Dept. of Physics, University of Pittsburgh, PA.

Information about the carbon bonding environment (graphitic vs. carbidic) can be obtained from analysis of the C (KLL) AES lineshape. Carbon in graphite exhibits a peak at 240 eV, while carbon in α-SiC exhibits peaks at 247 and 253 eV.

Results:

I) Surface Composition of α-SiC as a Function of Temperature and O_2 Pressure

A) Ultra-high vacuum

The α-SiC $(000\bar{1})$ surface composition was examined as a function of temperature from 300K to 1273K. Room temperature 400 eV Ar^+ bombardment produced a disordered surface with an I(C)/I(Si) AES ratio of 0.90 and trace amounts of surface oxide. Heating to 673K for 5 minutes increased the ratio to 1.20 due to adsorption of oxygen on the surface, which caused a decrease in the silicon 89 eV AES intensity. (See fig. 3) The source of this surface oxygen appeared to be background H_2O and/or O_2 in the UHV system. Five minutes of heating at 1073K increased the I(C)/I(Si) ratio to 1.40 and removed most of the surface oxide, suggesting SiO_x sublimation from the surface. Mass spectral analysis showed an increase in the 44 amu signal, which was attributed to SiO. Heating to 1198K for two minutes increased the I(C)/I(Si) ratio to 1.70 with no increase in the oxygen AES intensity. At both 1073K and 1198K AES showed an increase in signal at approximately 240 eV, indicating graphite formation. Raising the temperature to 1273K for 15 min. resulted in the complete removal of silicon from the surface region according to AES. The acceleration of the surface graphitization at this temperature was attributed to Si sublimation from the surface region.

B) 10^{-8} torr of O_2

The initial growth of oxide on α-SiC was examined at 300K using an O_2 pressure of 10^{-8} Torr. Prior to O_2 exposure, the sample was Ar^+ sputtered at 940K and then annealed for 15 minutes at 880K. Exposure to O_2 produced a monotonic decline in the silicon and carbon AES intensities. (See fig. 4) Lineshape analysis of the silicon and carbon AES signal after O_2 exposure showed the adsorbed oxygen was bonded to surface silicon atoms, not carbon. The intensity of the Si 89 eV AES transition after O_2 exposure showed the surface oxide produced was not SiO_2; however, AES was unable to determine the exact nature of the oxide. (See fig. 5) The decrease in the Si 89 eV AES intensity showed the surface exhibited a relatively fast initial rate of oxygen adsorption, but then showed a slower adsorption rate with increasing O_2 exposure. The experiment repeated at temperatures up to 833K produced similar results to those found at 300K. At all temperatures examined, the α-SiC surface appeared to approach a submonolayer oxidation limit with increasing O_2 exposure. In all cases the temperature during O_2 exposure was low enough such that Si and SiO sublimation from the surface did not occur, and hence surface graphitization did not occur. Heating the sample to 1100K in UHV after O_2 exposure removed the surface oxide via SiO sublimation, leaving behind surface graphite.

C) 1 atmosphere of O_2

X-Ray Photoelectron Spectroscopy was utilized to better determine the nature of the initial oxide formed on α-SiC by O_2 exposure. Alpha SiC cleaned by 3 kV Ar^+ bombardment at room temperature exhibited a C 1s and Si 2p binding energy (B.E.) of 283.0 and 100.0 eV, respectively. Oxidation of the

sample was performed by exposure to air for 25 minutes at room temperature. After exposure, the Si 2p peak showed a higher binding energy shoulder, attributed to the presence of oxidized silicon. A computer fitting of the experimental results assumed two types of silicon; oxidized and non-oxidized. (see fig. 6) The oxidized silicon exhibited a 2p B.E. of 100.8 eV, which is too low to be SiO_2 (Si 2p B.E. = 103.4 eV) [8]. The oxygen bonding to the α-SiC surface created a silicon oxidation state similar to that found in hexamethyldisiloxane ($(CH_3)_3SiOSi(CH_3)_3$; Si 2p B.E. = 100.9 eV) [8]. In this compound, oxygen is bonded between two silicon atoms, which are in turn bonded to 6 carbon atoms. This type of Si-O-Si bonding is a reasonable model for the initial oxide found on α-SiC.

The composition of the {0001} surfaces of an α-SiC single crystal after exposure to 1 atm of O_2 at various temperatures was examined via SAES. Figure 7 shows the composition of the (0001) surface after one hour O_2 exposure at several temperatures. Exposure to O_2 at 300K and 573K did not produce surface SiO_2, while O_2 exposure from 873K to 1373K did produce SiO_2. As expected, the average SiO_2 thickness increased with increasing temperature (120 Å SiO_2 at 873K vs. 1250 Å SiO_2 at 1373K). The presence of carbon within the SiO_2 layer was not detected by SAES. At each temperature examined, no significant difference in surface composition existed between the (0001) and $(000\bar{1})$ surface of the crystal. However, the SiO_2 overlayer produced on the $(000\bar{1})$ surface was 1.3 times thicker on average than the SiO_2 layer on the (0001) surface.

In order to determine if the difference in oxidative behavior seen between the {0001} surfaces was sample dependent, four α-SiC samples (2 Lely, 2 commercial) were exposed to 1 atm of flowing O_2 at 1323K for one hour. It was found with each crystal that the $(000\bar{1})$ surface produced, on average, a

thicker SiO_2 layer than the (0001) surface under the same conditions. However, the difference in oxide thickness between the two surfaces of the same crystal was far less dramatic than reported by Harris and Call. The thickness of the oxide produced and the difference between the two {0001} surfaces also appeared to be sample dependent. (See table 1) Argon ion depth profiling coupled with SAES revealed the SiO_2 thickness could vary considerably over each basal surface. No obvious differences between the Lely and commercial samples were observed.

II) The Role of Surface Defects in the O_2 Oxidation of α-SiC

The results cited above suggest that the polarity of the α-SiC {0001} surfaces alone is not as dominating a factor for O_2 oxidation as previously reported. In order to explore how sample annealing prior to 10^{-8} Torr O_2 exposure affected the interaction of O_2 with α-SiC, two different surface preparations with the same commercial α-SiC crystal were utilized. In case 1), the sample was sputtered at 923K for 15 minutes, quickly cooled to 773K, and then exposed to O_2. This will be referred to as the nonannealed surface. In case 2), the sample was sputtered under identical conditions, annealed in UHV at 923K for 15 minutes, then cooled to 773K and exposed to O_2. This will be referred to as the annealed surface.

The sputtered, nonannealed surface reacted with O_2 more extensively than the sputtered, annealed surface, illustrated in fig. 8. Interestingly, the carbon AES intensity of the nonannealed surface (not shown in fig. 8) showed a 26% decline with only 6 L O_2 exposure. This abrupt decline indicated Ar^+ sputtering produced reactive surface carbon that was removed to the gas phases by O_2. The reactivity of this carbon appeared to be removed during

annealing at 923K. In both cases the surface still showed a two-stage oxidation process similar to that seen with O_2 exposure of α-SiC at 300K.

The interaction of an ordered $(000\bar{1})$ surface with O_2 was examined at 973K. This temperature was chosen to maximize the surface oxidation rate while simultaneously avoiding SiO sublimation from the surface region. Exposure of the ordered (1x1) surface to 10^{-8} Torr O_2 produced much slower surface oxidation than seen with the poorer quality crystals used previously. After 6,700 L O_2 the silicon and carbon AES intensities had declined 22% and 11%, respectively. (See fig. 9) The (1x1) LEED pattern did not change with O_2 exposure; rather, it became sharper due to annealing at 973K during the O_2 exposure. This result suggested oxygen was bonding on steps or other defects.

Discussion:

I) Surface Composition of α-SiC as a Function of Temperature and O_2 Pressure

The UHV composition of the sputtered α-SiC $(000\bar{1})$ surface as a function of temperature changed due to surface oxide formation and sublimation of Si and SiO. Room temperature Ar^+ sputtering roughened the surface, making it highly susceptible to oxidation by background O_2 and/or H_2O. Lineshape analysis of the silicon AES signal showed that the oxide formed was not SiO_2. The surface oxide began to be removed at approximately 1100K, due to SiO sublimation from the surface region, which left behind graphitic surface carbon. At 1100K, the overall silicon AES intensity decreased, but analysis of the peak lineshape showed the silicon remaining on the surface was bonded to considerably less oxygen than before. This showed the changes in I(C)/I(Si) and I(O) were not due simply to a deposition of carbon on the surface. The sublimation of SiO at approximately 1100K has also been proposed and utilized

by Kaplan as a method of removing surface oxide from SiC [9]. The graphitization of the surface was further accelerated at 1273K due to silicon sublimation from the surface region. Mass spectroscopic studies of the high temperature decomposition of α-SiC have shown that $Si_{(g)}$ is clearly the dominate species found over α-SiC at thermodynamic equilibrium [10]. The $Si_{(g)}$ is produced via the reaction

$$\alpha\text{-SiC} \longrightarrow Si_{(g)} + C_{(graphite)} \quad \Delta H^{o}_{298} = 125 \text{ kcal/mole}$$

It is believed that as the graphite layer increases in thickness, the diffusion of silicon from the bulk to the surface dominates the sublimation process.

For comparison, Muehlhoff et al. reported that the surface composition of a sputtered $(000\bar{1})$ surface was stable up to 900K, at which carbon enrichment of the surface region took place. Further graphitization occurred at 1300K due to silicon sublimation from the surface region. One possible explanation for the differences in our results is that Muehlhoff's studies were done with a lower chamber pressure ($P<10^{-9}$ Torr vs. $P=2x10^{-9}$ Torr), which would slow the formation of surface oxides.

Exposure of sputtered, annealed α-SiC to 10^{-8} Torr O_2 from 300K to 833K produced a submonolayer surface oxide. In all cases the surface showed a two-stage oxidation process; a fast initial reaction with O_2 followed by a slower oxidation process with increasing O_2 exposure time. This type of oxygen adsorption has also been observed on single crystal Si (111) [11] and on room temperature α-SiC (0001) [12]. At these temperatures, the O_2 exposure did not produce SiO_2 and surface graphitization due to Si and SiO sublimation did not occur. Heating this submonolayer surface oxide to 1100K in UHV removed the oxide via SiO sublimation, leaving behind graphitic surface carbon.

$$\alpha\text{-SiC} + 1/2\ O_2 \longrightarrow SiO_{(g)} + C_{(graphite)}$$

The inability to obtain any LEED results from the basal surface used in these experiments indicated the surface was completely disordered. The orientation of the surface was not determined via Na_2CO_3 etching, since the oxidation results could not be attributed to a specific surface structure.

While α-SiC in low O_2 pressures and at elevated temperatures exhibits surface graphitization, the exposure of α-SiC to air or 1 atm O_2 produces surface silicon oxide (SiO_x) layers. Exposure of Ar^+ sputtered α-SiC to air for 25 minutes produced oxidized silicon with a fitted Si 2p B.E. of 100.8 eV, which suggested oxygen atoms were bridging surface silicon atoms. The model that the oxygen was bridging two silicon atoms, which were in turn bonded to carbon was based on a comparison of our results to reported XPS results for various organosilicon compounds. This type of bridging oxygen has also been proposed with single crystal Si [13] and β-SiC [14]. These binding energies are independent of the surface orientation utilized, since it appears that Ar^+ bombardment at room temperature disorders the surface, removing the "memory" of the surface polarity.

The production of SiO_2 from α-SiC and O_2 is extremely exothermic

$$\alpha\text{-SiC} + 3/2\ O_2 \text{------>}\ SiO_{2\ (amorphous)} + CO \quad \Delta H^o_{298} = -227\ \text{kcal/mole}$$

Therefore, the often cited resistance of SiC to oxidation should be attributed to kinetic factors. In our experiments, exposure of α-SiC {0001} surfaces to 1 atm O_2 for 1 hour at 300K and 573K did not produce SiO_2, while SiO_2 was produced from 873K to 1373K. The thickness of the SiO_2 surface layer produced in one hour on both {0001} surfaces increased with oxidation temperature. Carbon was not detected by SAES in the SiO_2 surface layers. This is consistent with previous gas chromatographic results, which suggested CO and/or CO_2 gas are the only C/O species formed during SiC oxidation in O_2 or air [15]. It has been

proposed that with thicker SiO_2 surface layers, the diffusion of the by-product CO through the SiO_2 layer determines the overall oxidation rate [5].

The exposure of four different α-SiC crystals at 1323K to 1 atm of flowing O_2 for one hour produced a wide range of surface oxide thicknesses. On each crystal the $(000\bar{1})$ surface produced a thicker SiO_2 surface layer than the (0001) surface. However, the difference between the two {0001} surfaces appeared sample dependent. In addition, the thickness of the SiO_2 layer on each basal surface varied over the area of the surface. These results suggest that the crystallographic polarity of α-SiC alone does not dominate the oxidation of the {0001} surfaces as significantly as previously reported.

It is reasonable to expect that an ideal, C-terminated $(000\bar{1})$ surface of α-SiC would show different oxidation characteristics than an ideal, Si-terminated (0001) surface during the growth of the first oxide layer. This could be attributed to the fact that oxygen bonded to the surface of SiC bonds only to silicon, not to carbon. However, it is expected that as the oxide layer increases in thickness, the sharpness of the SiO_2/SiC interface would be diminished . This would lead to the production of a Si/C/O interfacial region between the SiO_2 overlayer and the SiC substrate. Once this Si/C/O interface forms, the "memory" of the underlying crystal polarity is lost, and the two {0001} surfaces would be expected to produce SiO_2 layers of similar thickness under identical oxidative conditions.

The question remaining is why different α-SiC crystals produce SiO_2 layers of significantly different thicknesses and uniformity under identical high temperature O_2 exposures. Our work has shown that the oxidation of α-SiC surfaces is enhanced by the presence of surface defects. One possible explanation for the different oxidation characteristics of the {0001} surfaces is that as-grown $(000\bar{1})$ surfaces of α-SiC possess a higher density of steps, kinks,

or other defects than the (0001) surfaces. This would cause the $(000\bar{1})$ surface to oxidize faster than the (0001) surface initially, but would not be a significant factor as the oxide layer increased in thickness. In addition, if the density of defects was not uniform across a basal surface, it is reasonable to conclude the SiO_2 layer produced on that surface would not be uniform.

II) The Role of Surface Defects in the Oxidation of α-SiC by O_2

The studies performed at 773K showed that sputtered α-SiC surfaces exhibited a fast initial reaction with O_2, but then a slower oxidation process took over with increasing O_2 exposure time. The surfaces that were not annealed after Ar^+ bombardment were found to oxidize faster and more extensively than surfaces that did receive post-sputtering annealing. These nonannealed and presumably more disordered surfaces still showed a two-stage oxidation process with O_2 at 10^{-8} Torr. Argon ion bombardment produced highly reactive surface carbon, the reactivity of which was reduced by post-sputtering annealing. The susceptibility of SiC to ion bombardment damage has been documented. Studies of SiC subjected to 10 kV He^+ bombardment at room temperature have shown that SiC becomes flaky and porous on a micron scale, while SiC at 870K does not show bombardment damage [16].

The importance of surface defects in the oxidation of α-SiC by O_2 was dramatically shown by the interaction of O_2 with an ordered $(000\bar{1})$ surface at 973K. This ordered surface showed far less reactivity towards O_2 than the sputtered, disordered surfaces discussed previously. The low reactivity can be attributed in part to the fact that oxygen bonded to the surface of SiC bonds only to silicon atoms. In an ideal $(000\bar{1})$ surface, the topmost silicon atoms are in the second atomic layer and have no unsaturated bonds. Hence, the $(000\bar{1})$ surface would not be expected to react extensively with O_2. This is supported

by the fact that the (1x1) LEED pattern was not diminished by the O_2 exposure; rather, it became sharper due to annealing at 973K during the experiment. However, on an ideal α-SiC $(000\bar{1})$ surface the terminating atomic layer is composed only of carbon, with each carbon atom bonded to only three underlying silicon atoms. A surface terminated with unsaturated carbon bonds would be expected to be unstable, and yet the (1x1) LEED pattern of the $(000\bar{1})$ surface has been reported from 523K [17] to 1173K [18]. One possible explanation for the apparent stability of the ordered $(000\bar{1})$ surface in UHV up to 1173K is that the topmost carbon atoms are H-terminated. An analogous system is diamond (111), which is hydrogen terminated in UHV and exhibits a (1x1) LEED pattern up to approximately 1270K, at which point hydrogen desorption occurs [19].

Conclusions:

This work utilized a wide temperature and O_2 pressure range in order to study the surface oxidation process of α-SiC from the initial stages of oxide growth to the production of thick SiO_2 layers. In UHV, a sputtered α-SiC surface showed carbon enrichment due to sublimation of SiO and Si at approximately 1100K and 1270K, respectively. Exposure of sputtered α-SiC to 10^{-8} Torr O_2 from 300K to 833K resulted in a two stage oxidation process; a fast initial reaction with O_2 followed by a slower oxidation process with increasing O_2 exposure time. At all temperatures the O_2 exposure did not produce SiO_2 and surface graphitization due to SiO and Si sublimation did not occur. Surfaces that were not annealed after sputtering were found to oxidize faster and more extensively than surfaces that did receive post-sputtering annealing. This result, coupled with the low reactivity

of an ordered $(000\bar{1})$ surface towards O_2, indicate the importance of surface defects in the initial oxidation of SiC.

Exposure of α-SiC crystals to 1 atm O_2 for one hour produced surface silicon oxide layers. Exposure of α-SiC to O_2 at 300K and 573K resulted in the production of thin SiO_x (x<2) surface layers. From 873K to 1373K, SiO_2 surface layers were produced on both {0001} surfaces, with the SiO_2 production rate increasing with increasing O_2 exposure temperature. For α-SiC, the $(000\bar{1})$ surface was found to produce a thicker SiO_2 layer than the (0001) surface. However, the difference between the two {0001} surfaces appeared sample dependent and was not as dramatic as previously reported. In addition, the thickness of the SiO_2 surface layer showed considerable variation over the area of the basal surface. One possible explanation for these results is that as-grown α-SiC $(000\bar{1})$ surfaces possess a higher density of surface defects than (0001) surfaces. These defects enhance the oxidation process, causing the $(000\bar{1})$ surface to initially oxidize faster than the (0001) surface.

Acknowledgement:

The authors would like to thank Dr. Miquel Salmeron of Lawrence Berkeley Laboratory and Dr. R. Kaplan of the Naval Research Laboratory, Washington D.C. for their helpful discussions. J.M.P. would like to thank AT&T for the award of a Ph.D. fellowship during which this work was performed.

This work was supported by the Director, Office of Energy Research, Office of Basic Energy Sciences, Materials Sciences Division, of the U.S. Department of Energy under Contract No. DE-ACO3-76FOOO98.

References:

[1] S. Nishino, J. A. Powell, H. Will, Appl. Phys. Lett., 42(5), 460, (1983)

[2] S. Nishino, Y. Hazuki, H. Matsunami, T. Tanaka, J. Electrochem. Soc., 127, 2674, (1980)

[3] K. Brack, J. Appl. Phys., 36(11), 3560, (1965)

[4] Harris and Call in *Silicon Carbide 1973*, edited by R. Marshall, J. Faust, Jr., and C. Ryan (Univ. of South Carolina Press, Columbia, 1974) p. 329

[5] A. Suzuki, H. Matsunami, T. Tanaka, J. Electrochem Soc., 125, 1897, (1978)

[6] L. Muehlhoff, W. J. Choyke, M. J. Bozack, J. Yates, Jr., J. Appl. Phys., 60(8), 2842, (1986)

[7] L. Muehlhoff, M. J. Bozack, W. J. Choyke, J. Yates, Jr., J. Appl. Phys., 60(7), 2558, (1986)

[8] C. Wagner, W. Riggs, L. Davis, J. Moulder, *Handbook of X-Ray Photoelectron Spectroscopy*, (Perkin-Elmer Corp., Physical Electronics Div., Eden Prairie, MN, 1979)

[9] R. Kaplan, Surface Sci., 215, 111, (1989)

[10] J. Drowart, G. De Mani, M. Inghram, J. Chem. Phys., 29(5), 1015, (1958)

[11] C. Carosella, J. Comas, Surface Sci., 15, 303, (1969)

[12] B. Jorgensen, P. Morgen, J. Vac. Sci. Technol. A, 4(3), 1703, (1986)

[13] X. Zheng, P. Cao, Surface Sci. Lett., 219, L543, (1989)

[14] V. Bermudez, J. Appl. Phys., 66(12), 6084, (1989)

[15] Fitzer and Ebi in *Silicon Carbide 1973*, edited by R. Marshall, J. Faust, Jr., and C. Ryan (Univ. of South Carolina Press, Columbia, 1974) p.320

[16] S. Miyagawa, Y. Ato, Y. Miyagawa, J. Appl. Phys., 53(12), 8697, (1982)

[17] A. Van Bommel, J. Crombeen, A. Van Tooren, Surface Sci., 48, 463, (1975)

[18] R. Kaplan, T. Parrill, Surface Sci. Lett., 165, L45, (1986)

[19] B. Pate, M. Oshima, J. Silberman, G. Rossi, I. Lindau, W. Spicer, J. Vac. Sci. Technol. A, 2(2), 957, (1984)

Fig. 1: Ideal SiC single crystal structure (L. Muehlhoff et. al., J. Appl. Phys., 60(8), 2842 (1986))

Fig. 2: Na_2CO_3 etch patterns on the (0001) surface (a) and $(000\bar{1})$ surface (b). Magnification = 100x

Fig. 3: The α-SiC $(000\bar{1})$ surface composition in UHV as a function of temperature

Fig. 4: Variation in the AES intensities of α-SiC as a function of O_2 exposure at 300K

Fig. 5: AES spectra of a) clean α-SiC b) after 190L O_2 exposure at 300K c) clean SiO_2

Fig. 6: The Si 2p B.E. peak after exposing sputtered α-SiC to air for 25 minutes. The position of the peak maximum for SiO_2 is also shown.

Fig. 7: The α-SiC (0001) surface composition after exposure to 1 atm O_2 for 1 hour at various temperatures

Fig. 8: Variation in the I(O)/I(Si) AES ratio of α-SiC as a function of O_2 exposure at 773K. Note than sample annealing in UHV after Ar^+ sputtering reduces the chemisorption of surface oxygen.

Fig. 9: Variation in the AES intensities of an ordered α-SiC $(000\bar{1})$-(1x1) surface as a function of O_2 exposure at 973K

TABLE 1

Oxidation of α-SiC: 1 atm O_2, 1323K, 60 min

Crystal	Surface	Oxide Thickness (Å) by AES Depth Profiling		
		Ave.	Crystal Edge	Center of Crystal
α-SiC #1	$(000\bar{1})$	820	890	760
	(0001)	390	410	330
α-SiC #2	$(000\bar{1})$	720	740	770
	(0001)	290	320	280
α-SiC #3	$(000\bar{1})$	840	760	950
	(0001)	540	480	600
α-SiC #4	$(000\bar{1})$	780	820	740
	(0001)	640	820	460
Si	(111)	1270		

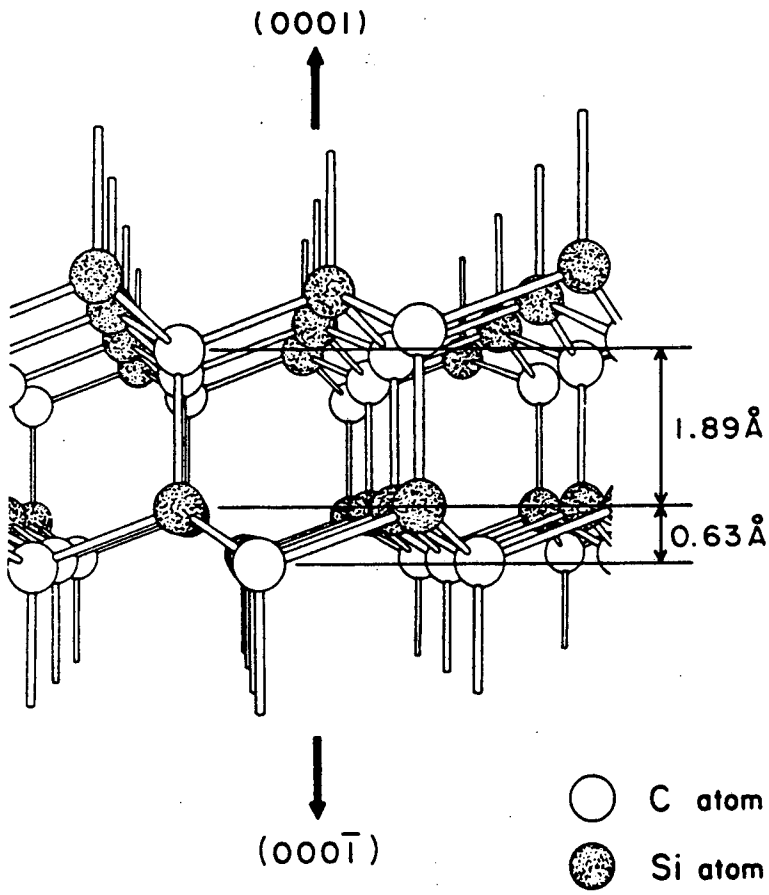

Fig. 1

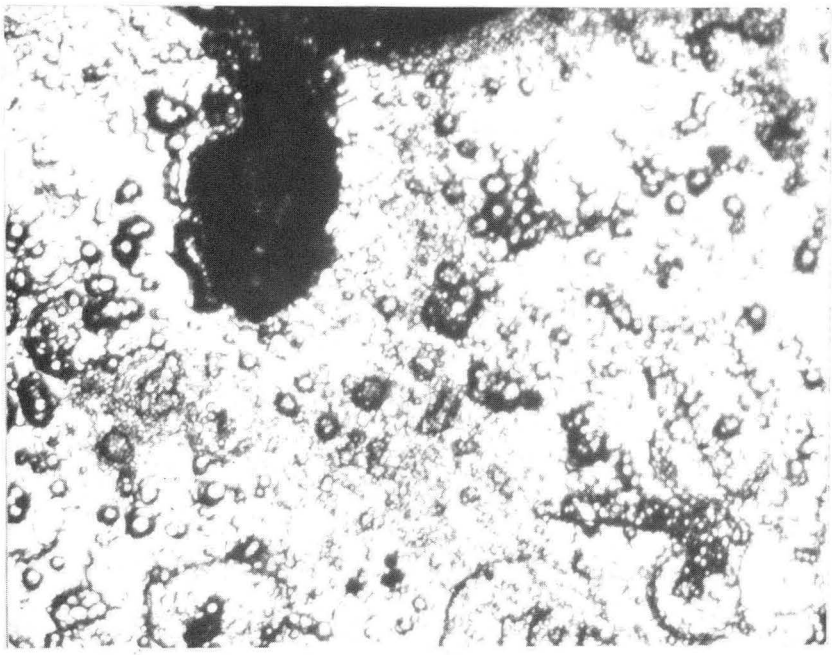

Fig. 2a
The (0001) Surface

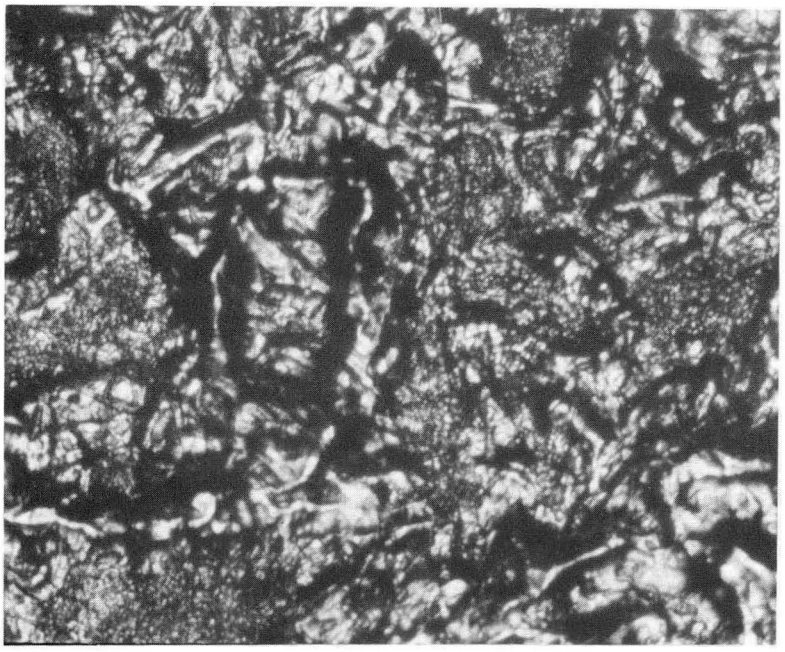

Fig. 2b
The $(000\bar{1})$ Surface

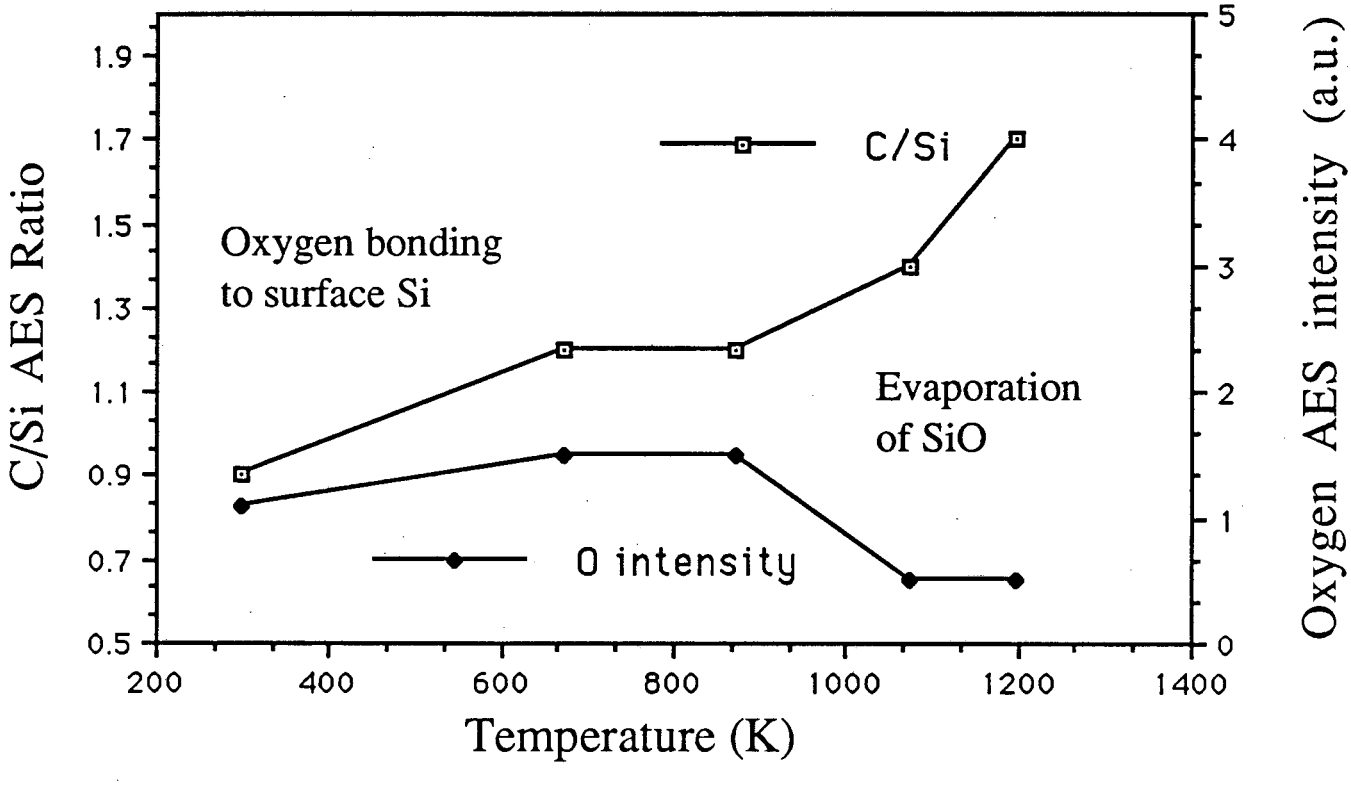
C/Si AES Ratio
1.9
1.7
1.5
1.3
1.1
0.9
0.7
0.5
200
400
600
800
1000
1200
1400
Temperature (K)
Oxygen AES intensity (a.u.)
5
4
3
2
1
0
C/Si
O intensity
Oxygen bonding
to surface Si
Evaporation
of SiO

Fig. 3

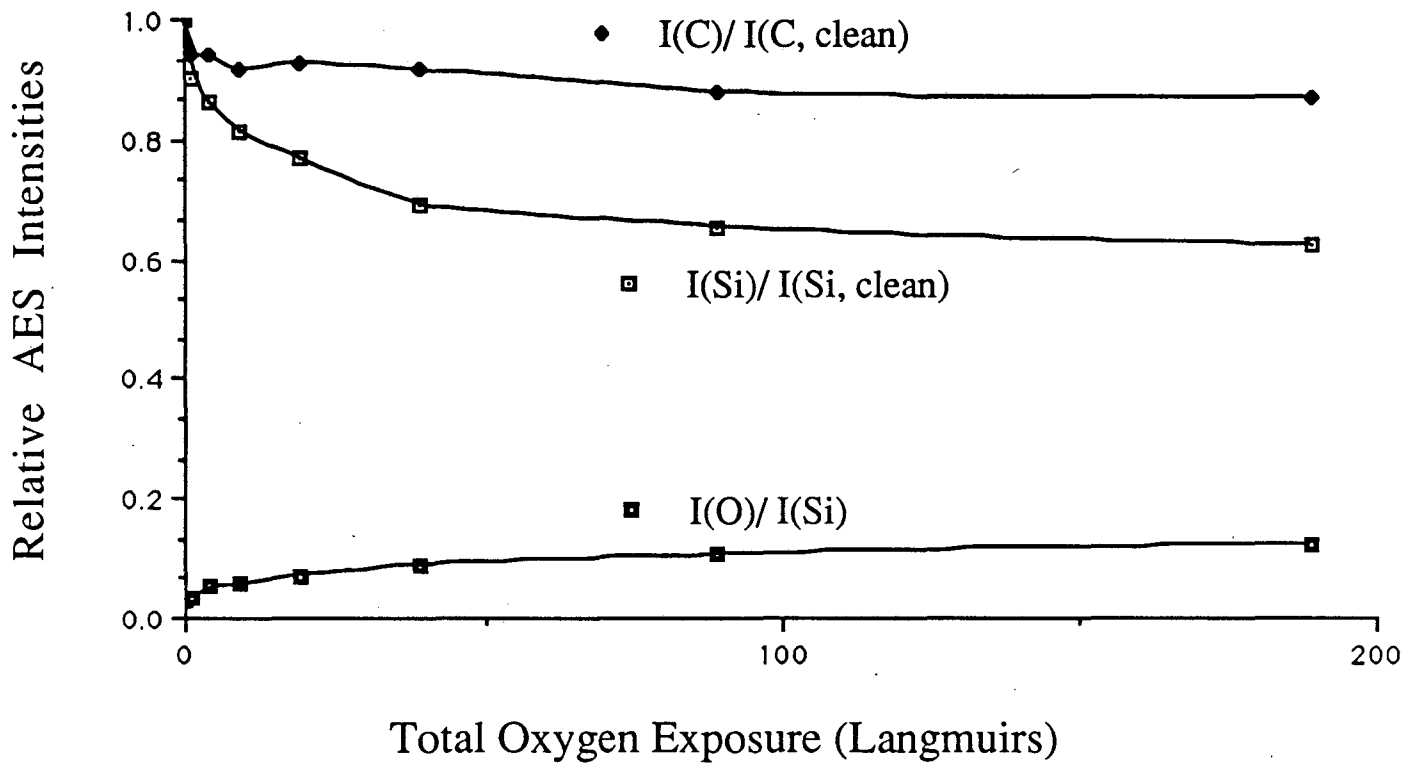
1.0
0.8
0.6
0.4
0.2
0.0
0
100
200
I(C)/ I(C, clean)
I(Si)/ I(Si, clean)
I(O)/ I(Si)
Relative AES Intensities
Total Oxygen Exposure (Langmuirs)

Fig. 4

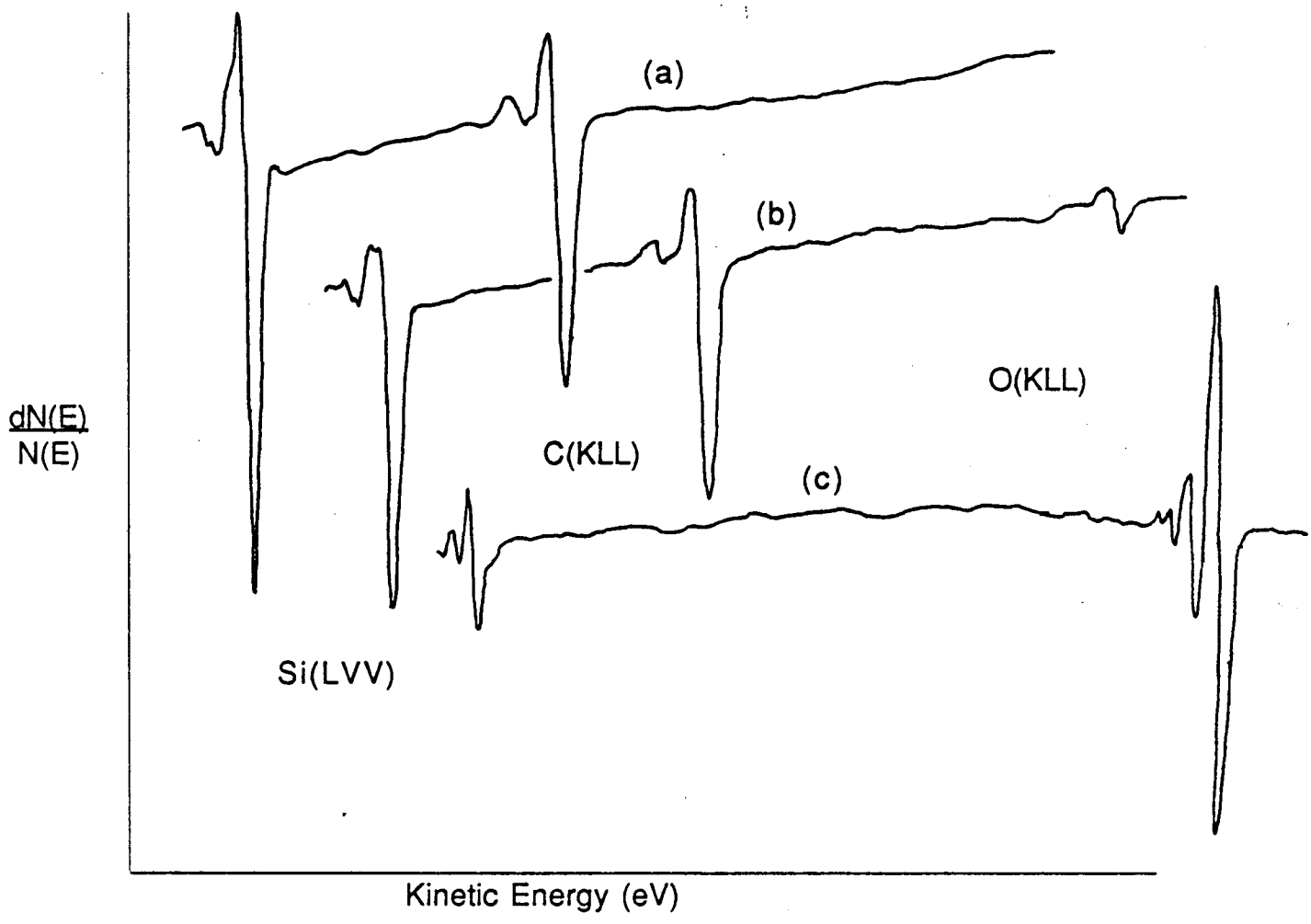

Fig. 5

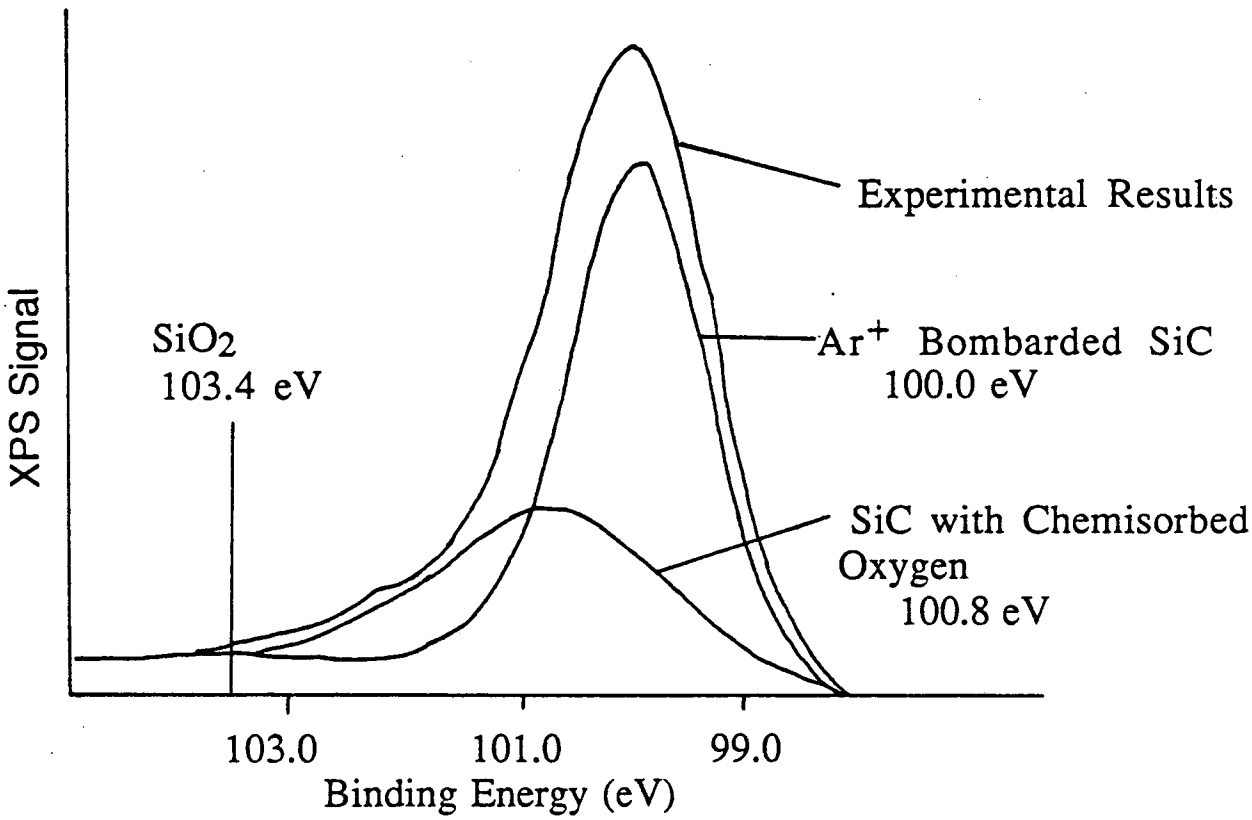
XPS Signal
SiO2
103.4 eV
Experimental Results
Ar+ Bombarded SiC
100.0 eV
SiC with Chemisorbed
Oxygen
100.8 eV
103.0
101.0
99.0
Binding Energy (eV)

Fig. 6

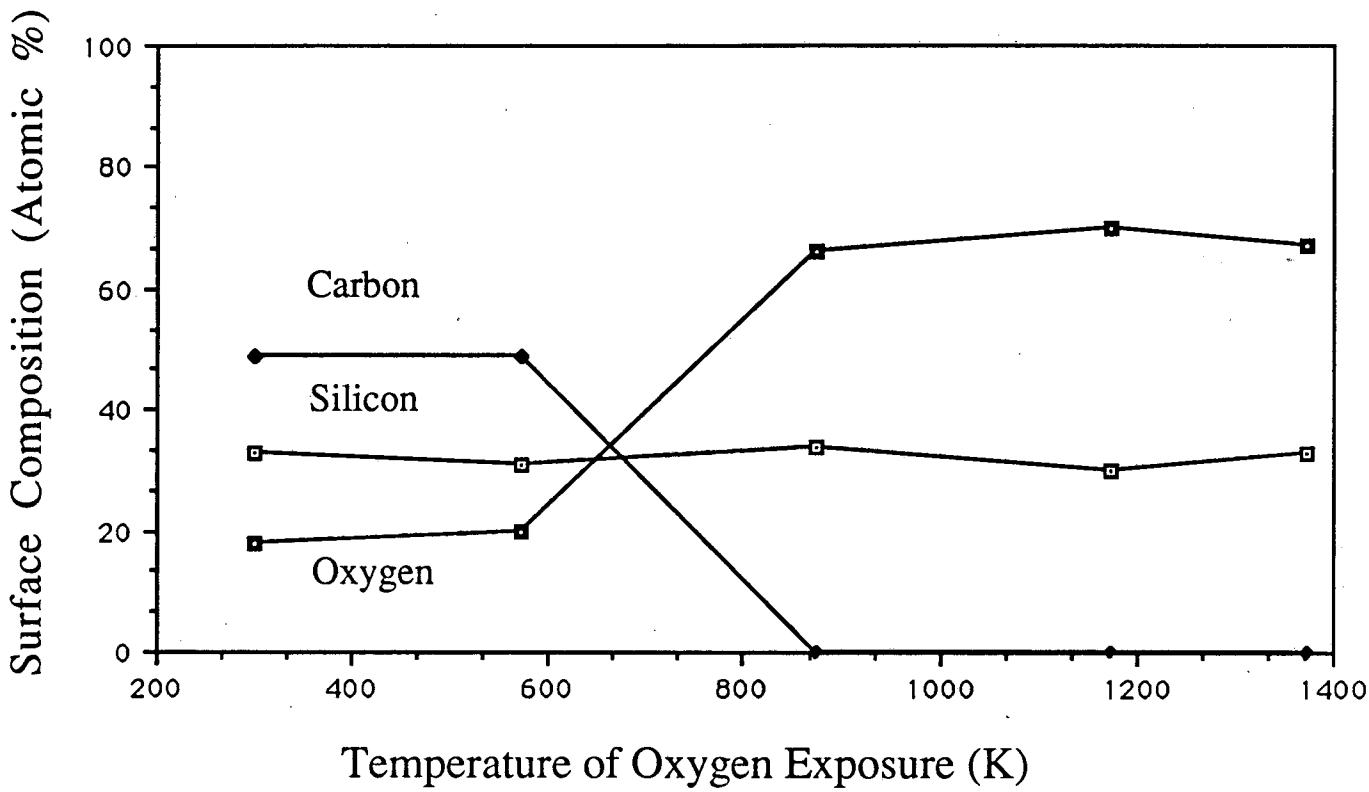
Surface Composition (Atomic %)
100
80
60
40
20
0
Carbon
Silicon
Oxygen
200
400
600
800
1000
1200
1400
Temperature of Oxygen Exposure (K)

Fig. 7

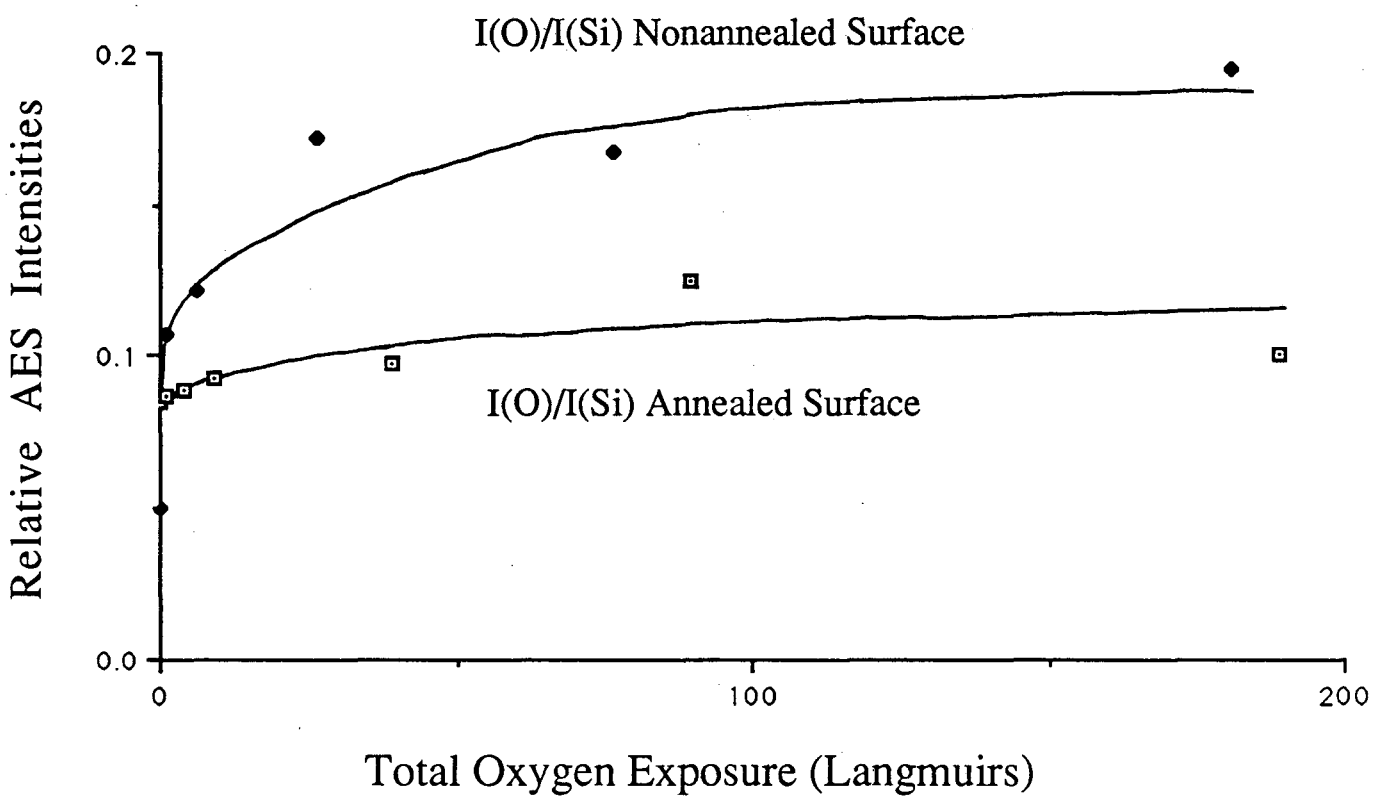
I(O)/I(Si) Nonannealed Surface
I(O)/I(Si) Annealed Surface
Relative AES Intensities
0.2
0.1
0.0
0
100
200
Total Oxygen Exposure (Langmuirs)

Fig. 8

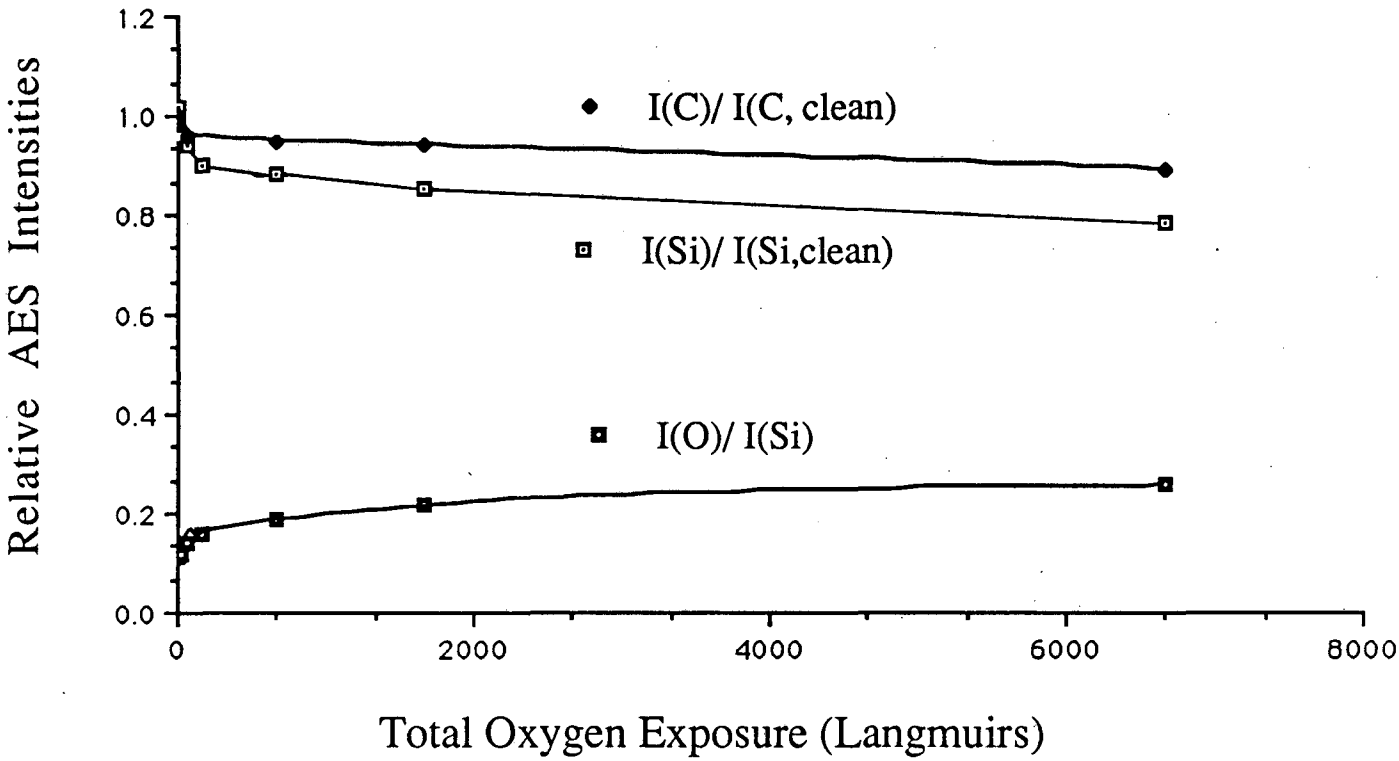
1.2
1.0
0.8
0.6
0.4
0.2
0.0
Relative AES Intensities
I(C)/ I(C, clean)
I(Si)/ I(Si,clean)
I(O)/ I(Si)
0
2000
4000
6000
8000
Total Oxygen Exposure (Langmuirs)

Fig. 9

LAWRENCE BERKELEY LABORATORY
CENTER FOR ADVANCED MATERIALS
1 CYCLOTRON ROAD
BERKELEY, CALIFORNIA 94720